JOURNAL OF NANO- AND ELECTRONIC PHYSICS
Vol. 10 No 1, 01005(5pp) (2018)

ЖУРНАЛ НАНО- ТА ЕЛЕКТРОННОЇ ФІЗИКИ
Том 10 № 1, 01005(5cc) (2018)

Modeling the Effects of Temperature and Doping Density on the Performance of Mid-infrared Quantum Cascade Lasers

D. Sebbar[1,2,*], B. Boudjema[1,†]

[1] LRPCSI, Université 20 août 1955-Skikda, B.P. 26, Route d'El-Hadaiek, 21000 Skikda, Algeria
[2] Laboratoire de Physique des Techniques Expérimentales et Applications de Médéa (LPTEAM), Université de Médéa, 26000 Médéa, Algeria

(Received 03 October 2017; revised manuscript received 13 November 2017; published online24 February 2018)

In this paper, we present the effects of temperature and doping density on the performance of mid-infrared quantum cascade lasers of three-level system based on rate equation. With taking into account the thermally activated population of the lower and upper lasing states. The theoretical study based on rate equation model leads to evaluation the dependence of the threshold current density and output power with temperature and sheet doping density with $n_s = 4.1$, 5.2 and 6.5×10^{11} cm^{-2}. This model allowed us to evaluate the shift of the energy difference between the upper and lower state with the variation the doping density. The results also show that output power is decreased when the temperature and the doping density are increased. The obtained results by the theoretical calculations are in good agreement with the experimental data, the results obtained from this study can be useful to improve the performance of the quantum cascade lasers.

Keywords: Quantum cascade laser, Rate equations, Effect of temperature, Thermally activated population, Sheet doping density, Threshold current density, Output power.

DOI: 10.21272/jnep.10(1).01005 PACS numbers: 42.55.Px, 42.55.Ah

1. INTRODUCTION

The quantum cascade lasers (QCLs) are unipolar devices based on tunneling and intersubband transitions, were proposed by R.F. Kazarinov and R.A. Suris in 1971 [1] and it was first realization by Faist et al, in 1994 [2]. These lasers have many applications in science and technology as chemical sensors [3], anesthetic gas detecting, pollution monitoring, free-space optical communication systems and infrared spectroscopy [4]. This kind of laser proved a large game of wavelengths ranging from 3 μm to 300 μm that not available in other lasers. The optimization of the quantum cascade lasers design was initially focused on obtaining devices operating at room temperature with low threshold current and increased output power.

Generally theoretical studies of QCLs performance is required to calculated electron energy levels and associated wave functions in a structure with taking into account the doping concentration of injector and it is analyzed by the Schrödinger-Poisson self-consistent equation[5]. An important aspect of QCL performance is its dependence on temperature, a variable applied electric field or an external magnetic field, extraction barrier, number of stage and injector doping concentration [6-13]. For other CaAs/AlGaAs plays a dominant role in preceding stimulated emission in the far-infrared rang which is the topic of investigation, both theoretical and experimental effort to improve the performance and efficiency of the QCLs. The modeling and optimization of QCLs depend mainly on the ability of controlling the doping, temperature, electric field.

In this paper we use the rate equation model to calculate the threshold current density and output power as a function of the temperature and the concentration density. We compare the results obtained by our theoretical model with experimental data available in literatures.

2. THEORETICAL CALCULATION

2.1 Rate Equations

The three-level system was based on rate equations material system used for describing the dynamic of carriers and photon numbers in each level for quantum cascade, where spontaneous emission can be neglected [14], and taking into account the thermally activated population in the lower and upper lasing state n_2^{therm} and state n_3^{therm} respectively.

$$\frac{dN_3}{dt} = \eta wL\frac{J}{e} - \frac{N_3 - WLn_3^{therm}}{\tau_3} - \Gamma\frac{C'\sigma_{32}}{V}(N_3 - N_2)N_{ph} \quad (1a)$$

$$\begin{aligned}\frac{dN_2}{dt} = (1-\eta)wL\frac{J}{e} + \Gamma\frac{C'\sigma_{32}}{V}(N_3 - N_2)N_{ph} - \\ -\frac{N_2 - WLn_2^{therm}}{\tau_{21}} + \frac{N_3 - WLn_3^{therm}}{\tau_{32}},\end{aligned} \quad (1b)$$

$$\frac{dN_{ph}}{dt} = N\Gamma\frac{C'\sigma_{32}}{V}(N_3 - N_2)N_{ph} - \frac{N_{ph}}{\tau_P}, \quad (1c)$$

where N_i is electron number in level i, is the photon number, $(1-\eta)J$ and ηJ are the current density injected into the lower and upper lasing level respectively, η is the injection efficiency, L and W are the length and width of the cavity respectively, V is the volume of the cavity determined by $V = NWLL_p$ where L_p in this case

*sebbardjamel@gmail.com
†boudjema_b@yahoo.fr

is the length of one period of the cascade laser structure, while N is the number of periods, e is the electron charge, τ_3, τ_2 are electron lifetime in the $n = 3$ and $n = 2$ respectively, τ_{21}, τ_{32} is electron scattering time between the states of the system, Γ is confinement factor, τ_p represent the photon lifetime in the cavity obeys the following relation $\tau_p^{-1} = c'(a_w + a_m)$ where $c' = c/n_{eff}$ is the velocity of light in structure (n_{eff} is the refractive index of the cascade laser structure), a_w is the waveguide losses while a_m is the mirrors losses determined by $a_m = -\ln(R_1R_2)/2L$ where R_1 and R_2 are represent the reflectivity of facet 1 and 2 respectively. σ_{32} is the stimulated emission cross section given by:

$$\sigma_{32} = \frac{4\pi e^2 z_{32}^2}{\varepsilon_0 n_{eff} \lambda \left(2\Upsilon_{32}(T)\right)}, \tag{2}$$

where z_{32} is the optical dipole matrix element of transition, λ is the QCL wavelength, ε_0 is the electric permittivity of free space T is the absolute temperature, $2\Upsilon_{32}(T)$ is the full width at half maximum FWHM, it's temperature dependence is given by:

$$\frac{\Upsilon_{32}(T)}{\Upsilon_{32}(77)} = \frac{2n_q(T)+1}{2n_q(77)+1}, \tag{3}$$

where $n_q(T)$: the phonon population, is determined by the Bose Einstein distribution:

$$n_q(T) = \frac{1}{\exp\left(\frac{\hbar\omega_{LO}}{KT}\right)-1}, \tag{4}$$

where $\hbar\omega_{LO}$ is the energy of the longitudinal optical phonon.

The population inversion $\Delta N = N_3 - N_2$ between upper and lower levels is determined by rate equations and it's given by:

$$\Delta N(T) = \frac{\left(\left(1-\frac{\tau_{21}(T)}{\tau_{32}(T)}\right)\eta - (1-\eta)\frac{\tau_{21}(T)}{\tau_3(T)}\right)\tau_3(T) WL\frac{J}{e} - WLn_2^{therm} + WLn_3^{therm}}{1+\frac{N_{ph}}{N_{ph},sat(T)}}, \tag{5}$$

where $N_{ph,sat}(T)$ is the saturation photon number in the cavity given by Hamadou et al. [14]:

$$N_{ph},sat(T) = \frac{V}{\Gamma C'\sigma_{32}\left(1+\frac{\tau_{21}(T)}{\tau_{31}(T)}+\frac{\tau_{21}(T)}{\tau_{th}}\right)\tau_3(T)}, \tag{6}$$

where $\tau_3^{-1} = \tau_{31}^{-1} + \tau_{32}^{-1} + \tau_{th}^{-1}$, and τ_{th} is the thermionic lifetime of a electron undera electrical field as defined in ref. [15]:

$$\tau_{th} = \left(\frac{2\pi m^* L_z^2}{KT}\right)\exp\left(\frac{\Delta E_{act}}{KT}\right), \tag{7}$$

where ΔE_{act} is the activation energy, m^* is the effective mass for the electron in the well, L_z is the approximate extent of the $n = 3$ state wave function and K is the Boltzmann constant.

The threshold current density relation can be determined by $\Delta N_{th} = V/N\Gamma c'\sigma_{32}\tau_p$ [16], where ΔN_{th} is obtained by put N_{ph} equals to zero and replacing J by J_{th} in the Eq. (5) we get the following relation:

$$j_{th} = \frac{1}{\left(\left(1-\frac{\tau_{21}(T)}{\tau_{32}(T)}\right)\eta-(1-\eta)\frac{\tau_{21}(T)}{\tau_3(T)}\right)\tau_3(T)} \times \left[\frac{\varepsilon_0 n_{eff}\lambda L_p 2\Upsilon_{32}(\alpha_w+\alpha_m)}{4\pi e z_{32}^2\Gamma} + en_2^{therm} - en_3^{therm}\right]. \tag{8}$$

2.2 Thermally Activated Population

The thermally activated population of the upper state n_3^{therm} and the lower state n_2^{therm} play important role in the expression of the threshold current density. In a simplified model the thermal population n_3^{therm} and n_2^{therm} can be approximated by a simple thermal activation term at a temperature T and the sheet doping density of the injector n_s as following:

$$n_3^{therm} = n_s \exp\left(-\frac{\Delta_{3inj}}{KT}\right), \tag{9a}$$

$$n_2^{therm} = n_s \exp\left(-\frac{\Delta_{2inj}}{KT}\right), \tag{9b}$$

where Δ_{3inj} and Δ_{2inj} are the energy difference between the upper and lower state respectively and the chemical potential (quasi-Fermi level) of the injector. The threshold current density can be depend on the temperature and the doping injector as follow:

$$j_{th}(T,n_s) = j_{th}(T) + \frac{en_s\left(\exp\left(-\frac{\Delta_{2inj}}{KT}\right)-\exp\left(-\frac{\Delta_{3inj}}{KT}\right)\right)}{\tau_{eff}(T)} \tag{10}$$

with $\tau_{eff}(T) = \left(\left(1-\frac{\tau_{21}(T)}{\tau_{32}(T)}\right)\eta-(1-\eta)\frac{\tau_{21}(T)}{\tau_3(T)}\right)\tau_3(T)$,

where $\tau_{eff}(T)$ represent the effective lifetime, the first term $J_{th}(T)$ is calculated by model of Hamadou et al [14], given for the sheet density of the injector n_{s0} equals 4.1×10^{11} cm^2, so Eq. (10) become:

$$j_{th}(T,n_s) = j_{th}(T,n_{s0}) + \frac{en_s\left(\exp\left(-\frac{\Delta_{2inj}}{KT}\right)-\exp\left(-\frac{\Delta_{3inj}}{KT}\right)\right)}{\tau_{eff}(T)}. \tag{11}$$

By conformity of the Eq.11 with the relationship $J_{th}(N_s) \times (KA/cm^2) = J_{th}(4.1)+Y(N_s - 4.1)$ reported in ref.

[17], which gives the threshold current density depending on injector doping, we find that the first term $J_{th}(4.1)$ depends on the sheet density from the reference concentration n_{s0} and it is equals to 4.1 $10^{11}\,\text{cm}^{-2}$, while in the second term N_s represents the sheet density given in $10^{11}\,\text{cm}^{-2}$, Y is the constant. This conformity gives a system of two equations depends on the values of the temperatures T_1 and T_2 where their objective is to determine the values of the Δ_{2inj} and Δ_{3inj}, which is described as following:

$$\frac{en_s\left(\exp\left(-\frac{\Delta_{2inj}}{KT_1}\right)-\exp\left(-\frac{\Delta_{3inj}}{KT_1}\right)\right)}{\tau_{eff}\left(T_1\right)}=Y_1\left(N_s-4.1\right), \tag{12a}$$

$$\frac{en_s\left(\exp\left(-\frac{\Delta_{2inj}}{KT_2}\right)-\exp\left(-\frac{\Delta_{3inj}}{KT_2}\right)\right)}{\tau_{eff}\left(T_2\right)}=Y_2\left(N_s-4.1\right), \tag{12b}$$

where Y_1 and Y_2 are the constants extracted from the experimental results at the temperatures T_1 and T_2 respectively. The Eq.12 formed a system of nonlinear equations with two unknowns Δ_{3inj} and Δ_{2inj}, for $T_2/T_1 = 3$ and we assume that $x_1 = \exp(-\Delta_{3inj}/kT_2)$ and $x_2 = \exp(-\Delta_{2inj}/kT_2)$ this system leads to solving a quadratic equation as a flowing form:

$$3\alpha_2 X_1^2+3\alpha_2 X_1+\alpha_2^3-\alpha_1=0 \tag{13a}$$

and

$$X_2=\alpha_2+X_1 \tag{13b}$$

with take the expression of α_1 and α_2 as following:

$$\alpha_1=Y_1\left(N_s-4.1\right)\tau_{eff}\left(T_1\right)/en_s, \tag{14a}$$

$$\alpha_2=Y_2\left(N_s-4.1\right)\tau_{eff}\left(T_2\right)/en_s. \tag{14b}$$

We obtain the expression of Δ_{2inj} and Δ_{3inj} as follows:

$$\Delta_{2inj}=-KT_2Ln\left(X_2\right), \tag{15a}$$

$$\Delta_{3inj}=-KT_2Ln\left(X_1\right). \tag{15b}$$

In this model Δ_{3inj} and Δ_{2inj} represent the shift of the energy difference between both the upper and lower level and the chemical potential of the injector with the their exact values, so Δ_{3inj} and Δ_{2inj} are affected by the variation of doping concentration, where the exact values of Δ_{2inj} and Δ_{3inj} are include in first term of the threshold current density of the Eq.11. This allows us to replace Δ_{2inj} and Δ_{3inj} by $\Delta\Delta_{2inj}$ and $\Delta\Delta_{3inj}$ respectively. For example to calculate the exact value of the Δ_{2inj} based on the relationship as $V_p = (\hbar\omega + \Delta_{2inj})$ [18], where V_p is the voltage drop per period that can be expressed as $V_p = FL_p$, where F is the intensity of the electric field.

2.3 Output Power

Output power is related on the a number of photons and can be written by this relation:

$$P_{out}=\eta_0\hbar\omega Nph/\tau_p, \tag{16}$$

where $\hbar\omega$ is the energy of lasing laser, and η_0 is efficiency given by:

$$\eta_0=\frac{\left(1-R_1\right)\sqrt{R_2}}{\left(1-R_1\right)\sqrt{R_2}+\left(1-R_2\right)\sqrt{R_1}}\frac{\alpha_m}{\alpha_W+\alpha_m}. \tag{17}$$

3. RESULTS AND DISCUSSION

In this section we treat the dependences of the threshold current density and output power with the variation of the temperature and doping density for the structure reported in ref. [19]. In our numerical calculation we use the parameters at $T = 77$ K [14, 17, 20], some parameters can be varied with temperature as $\tau_{32} = 32$ ps, $\tau_{21} = 0.3$ ps, $\tau_3 = 1.4$ ps, $2\Gamma_{32} = 12$ meV and parameters fixed with temperature as $\lambda = 9$ µm, $Z_{32} = 1.7$ nm, $n_{eff} = 3.27$, $\alpha_w = 18$ cm^{-1}, $\alpha_m = 6$ cm^{-1}, $\Delta E_{act} = 58$ meV, $N = 48$, $\Gamma = 0.32$, $L_p = 45$ nm, $L_z = 10$ nm, $L = 1$ mm, $W = 34$ µm, $m^* = 0.067\, m_0$, $Y_1 = 0.91$ KA, $Y_2 = 2.91$ KA, $T_1 = 80$ k and $T_2 = 240$ k.

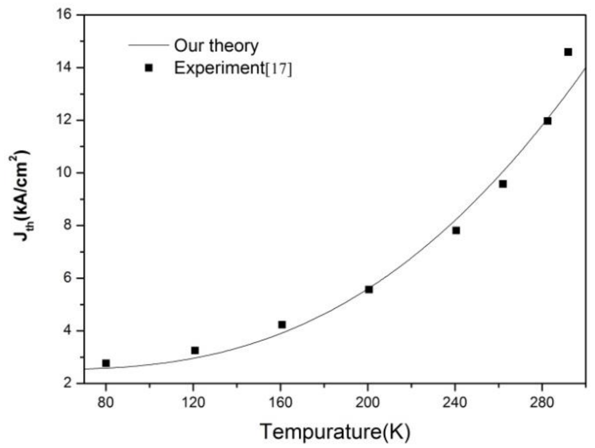

Fig. 1 – Variation of threshold current as a function of the temperature, it also shows comparison between our model and experimental data[17]

In Fig. 1 we plot the threshold current density as a function of temperatureas defined in Eq. 11 with doping density $n_s = 4.1 \times 10^{11}$ cm^{-2}, in this case the second term in Eq. 11 depend on the variation of doping density which vanish when $\Delta\Delta_{2inj}$ equals to the $\Delta\Delta_{3inj}$ and take the value of 7.49 meV, the model in this case is identical to the model reported by Hamadou et al. [14], our model shows that at $T = 292$ K we have 10.22 % error compared with the experimental results reported in ref. [17], this error due to the variation of fractional injection η where in our calculations takes the fixed value equals to one for various temperature values.

The dependence of the threshold current density with versus sheet doping density of the injector between 4.1 and 6.5×10^{11} cm^{-2} is plotted in Fig. 2, it shows clearly that the proportionality quasi linear of the threshold current density with the sheet doping density, for sheet doping density of the injector 5.2×10^{11} cm^{-2} we find $\Delta\Delta_{2inj} = 7.2$ meV and

$\Delta\Delta_{3inj}$ = 7.8 meV as for the sheet doping density of the injector 6.5×10^{11} cm^{-2} we find $\Delta\Delta_{2inj}$ = 6.98 meV and $\Delta\Delta_{3inj}$ = 8.3 meV. Also Fig. 2 shows a comparison between the theoretical and experimental results, we notice that for the temperature T = 240 K are in very good agreements, however for T = 80 K are in good agreements with small shift corresponding to the sheet doping density 6.5×10^{11} cm^{-2} this shift is probably due to the several parameters in our model taken fixe with the variation of the temperature, such as the wavelength, mode confinement factor, and the optical dipole matrix element of transition, where these parameters which expected to have a great impact on quantum cascade lasers performance.

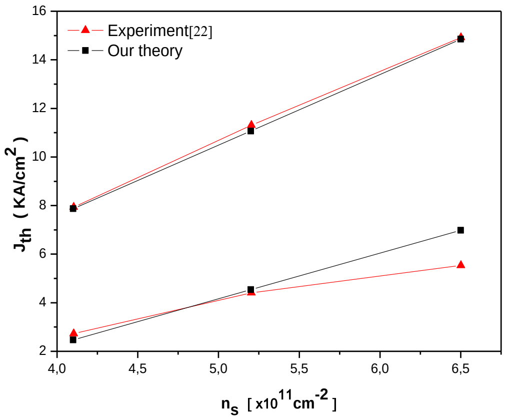

Fig. 2 – Variation of threshold current as a function of the Sheet doping density of the injector, it also shows comparison between our model and experimental data [17]

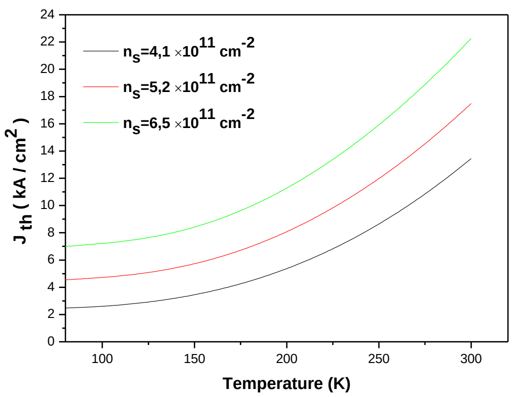

Fig. 3 – Variation of threshold current as a function of the temperature

Fig. 3 shows the variation of threshold current density as a function of temperature for different sheet doping density. The optical power of the injector between 4.1 and 6.5×10^{11} cm^{-2}, can be result that the threshold current density increase with the sheet doping density.

The optical power is plotted in Fig. 4 and Fig. 5 as a function of injection current for different sheet doping density at temperatures T = 80 K and T = 240 K respectively, therefore we noted that the optical power decrease with temperature and also with injection current and doping density.

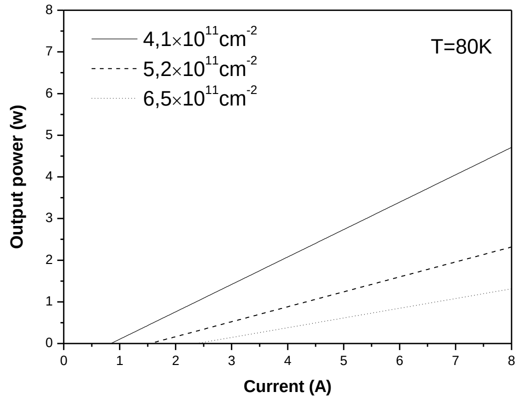

Fig. 4 – Variation of output power as a function of the injection current at T = 80 K

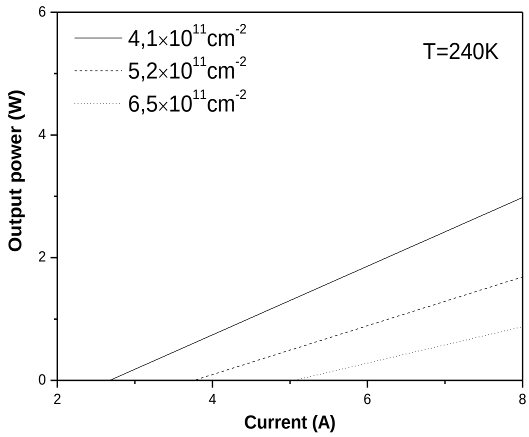

Fig. 5 – Variation of output power as a function of the injection current at T = 240 K

4. CONLUSION

In this paper the rate equation model have been used by taking into account the thermally activated population in the lower and upper lasing states in order to study the influence of both temperature and doping in performance of the quantum cascade lasers. Our numerical results show that the threshold current density increase with the temperature and doping density, however the output power decrease when the temperature and doping density increase. We have also estimated the shift of the energy difference between the upper and lower state with the variation the doping density. The validity of these results obtained by our model are in very good agreement with the experimental results.

AKNOWLEDGEMENTS

The authors are gratefully acknowledgethe Algerian Ministry of Higher Education for a research grant.

REFERENCES

1. R.F. Kazarinov, R.A. Suris, *Sov. Phys.-Semicond.* **5** No 4, 707 (1971).
2. J. Faist, F. Capasso, D.L. Sivco, C. Sirtori, A.L. Hutchinson, A.Y. Cho, *Science* **264**, 553 (1994).
3. C. Gmachl, F. Capasso, D.L. Sivco, A.Y. Cho, *Report. Progress Phys.* **64** No 11, 1533 (2001).
4. B.G. Lee, M.A. Belkin, R. Audet, J. MacArthur, L. Diehl, C. Pflugl, F. Capasso, *Appl. Phys. Lett.* **91** No 23, 231101 (2007).
5. K. Donovan, P. Harrison, R.W. Kelsall, *J. Appl. Phys.* **89** No 6, 3084 (2001).
6. F. Jerome, F. Capasso, D.L. Sivco, A.L. Hutchinson, C. Sirtori, S.N.G. Chu, A.Y. Cho, *Appl. Phys. Lett.* **65** No 23, 2901 (1994).
7. S. Saha, J. Kumar, *Infrared Phys. Technol.* **79**, 85 (2016).
8. H. Li, J.C. Cao, J.T. Lü, Y.J. Han, *Appl. Phys. Lett.* **92** No 22, 221105 (2008).
9. C. Gmachi, F. Capasso, A. Tredicucci, D.L. Sivxo, R. Kohler, A.L. Hutchinson, A.Y Cho, *IEEE J. Selected Topics in Quantum Electron.* **5** No 3, 808 (1999).
10. M. Giehler, R. Hey, H. Kostial, S. Cronenberg, T. Ohtsuka, L. Schrottke, H.T. Grahn, *Appl. Phys. Lett.* **82** No 5, 671 (2003).
11. V.D. Jovanović, D. Indjin, N. Vukmirović, Z. Ikonić, P. Harrison, E.H. Linfield, H.E. Beere, *Appl. Phys. Lett.* **86** No 21, 211117 (2005).
12. S. Hofling, V.D. Jovanovic, D. Indjin, J.P. Reithmaier, A. Forchel, Z. Ikonic, V. Milanovic, *Appl. Phys. Lett.* **88** No 25, 251109 (2006).
13. T. Aellen, M. Beck, N. Hoyler, M. Giovannini, J. Faist, E. Gini, *J. Appl. Phys.* **100** No 4, 43101 (2006).
14. A. Hamadou, J-L. Thobel, S. Lamari, *Opt. Commun.* **281** No 21, 5385 (2008).
15. H. Schneider, K.V. Klitzing, *Phys. Rev. B* **38** No 9, 6160 (1988).
16. A. Hamadou, S. Lamari, J.L. Thobel, *J. Appl. Phys.* **105** No 9, 093116 (2009).
17. V.D. Jovanović, S. Höfling, D. Indjin, N. Vukmirović, Z. Ikonić, P. Harrison, A. Forchel, *J. Appl. Phys.* **99** No 10, 103106 (2006).
18. C. Sirtori, J. Faist, F. Capasso, D.L. Sivco, A.L. Hutchinson, A. Cho, *Appl. Phys. Lett.* **69** No 19, 2810 (1996).
19. H. Page, C. Becker, A. Robertson, G. Glastre, V. Ortiz, C. Sirtori, *Appl. Phys. Lett.* **78** No 22, 3529 (2001).
20. V. Ortiz, C. Becker, H. Page, C. Sirtori, *J. Crystal Growth* **251** No 1, 701 (2003).